STANFORD RESEARCH INSTITUTE
MENLO PARK, CALIFORNIA

MEASUREMENT OF ENERGY FLUX DENSITY DISTRIBUTION IN THE FOCUS OF AN ARC IMAGE FURNACE

Rodney B. Beyer, Leonard McCulley, and Marjorie W. Evans

March 15, 1963

MEASUREMENT OF ENERGY FLUX DENSITY DISTRIBUTION IN THE FOCUS OF AN ARC IMAGE FURNACE

Rodney B. Beyer, Leonard McCulley, and Marjorie W. Evans

SUMMARY

A calorimeter for mapping flux density in a focal volume is described. The design is based on an earlier design by Broido and Willoughby. It differs chiefly in two ways. First it is much smaller in order to permit its placement inside a test specimen chamber. Second the design provides for an aperture-containing shield which is placed in front of the receiving surface calorimeter in order to limit the area of beam which is intercepted. The decay constant is 2×10^{-3} sec^{-1}. Flux densities ranging from 5 to 120 cal/cm^2-sec can be conveniently measured over intercepted beam areas of from 0.03 to 0.2 cm^2.

With this calorimeter the flux density distribution in the focal volume of a double ellipsoidal arc image furnace system was determined.

This research was supported by Stanford Research Institute under Project 004-531-236, and by the Office of Naval Research under Contract Nonr-3415(00).

The arc image furnace is a useful device for supplying energy at controllable flux density levels and for controllable times.[1,2] For example, in work soon to be published it has been used in studying the initiation of deflagration waves at solid surfaces. The radiation beam from the double-ellipsoidal carbon arc image furnace used in this work, shown schematically in Fig. 1, converges toward a 1-cm diameter focus in a cone with vertex angle of 120 degrees. Adjustable shutters (not shown in Fig. 1) placed near the sample reflector allow the magnitude of flux density at the focus to be adjusted. The focus is an ellipsoidal volume in which the flux density varies. For the furnace to be a useful instrument in a quantitative study, one must know the flux density distribution throughout this focal volume and especially the maximum flux density. The purpose of this work was to design a suitable calibrating calorimeter, and with it to map the flux density distribution.

1. Design

The calorimeter design was an adaptation of one by Broido and Willoughby.[3] The receiver was constructed from a copper disc, 0.10 cm thick and approximately 0.4 cm in radius. This was pressed into a spherical segment with an inner radius of 0.55 cm and an inner height of 0.15 cm. The inner surface was blackened with electro-deposited platinum black. A plane silver foil shield, 0.0127 cm thick, with an aperture which was varied between 0.025 and 0.508 cm in diameter, was placed in front of the concave surface to limit the area of the beam intercepted by the receiver. The shield was spaced 0.025 cm from the rim of the

receiver, with the line connecting the center of the aperture and the center of the receiver parallel to the optical axis of the system. A 5-mil copper-constantan thermocouple was silver-soldered to the back side of the receiver near one edge to measure the temperature rise. The receiver was mounted on Bakelite posts for thermal insulation from the holder and the plate containing the aperture. A sketch of the receiver and the shield is shown in Fig. 2. The physical constants of the receiver were

a = absorptivity = 0.97

ρ = density = 8.92 gm/cm^3

c = specific heat = 0.093 cal/$^\circ$C-gm

λ = thermal conductivity = 0.91 cal/cm-$^\circ$C-sec

κ = $\lambda/\rho\, c$ = thermal diffusivity = 1.095 cm^2/sec

δ = thickness = 0.10 cm

m = mass = 0.406 gm

2. Theory

If heat losses can be neglected, if the gradient across the thickness δ is small, and if the difference between the temperature measured at the edge and the average temperature is small, the average flux density I_a at the aperture over an aperture area A_a is given over any time interval Δt by

$$I_a = \frac{m\, c}{a\, A_a}\left(\frac{\Delta\theta_{AV}}{\Delta t}\right) \qquad (1)$$

where $\Delta\theta_{AV}$ is the increase of average temperature of the receiver, and the temperature may be measured anywhere on the calorimeter. The flux

density versus time curve of a pulse of energy is obtained by differentiating the temperature-time curve of the calorimeter.

Following Broido and Willoughby the characteristics of the calorimeter are defined in terms of (a) the decay constant Λ (sec^{-1}),

$$\Lambda = \frac{h}{A_c \rho c \delta} \tag{2}$$

where h is the heat loss coefficient of the receiver in cal/sec-^{0}C and A_c is the calorimeter surface area, and (b) a differentiated time constant T (sec),

$$T = \frac{1.7\delta^2}{K\pi^2} \tag{3}$$

They showed that if $\Lambda t/2 << 1$, heat losses can be neglected. Again following Broido and Willoughby h/A_c was estimated by assuming conductive heat losses to be negligible and convective heat losses to be equal to radiative losses, as calculated from the Stefan-Boltzmann law. In our measurements the calorimeter temperature rise was varied between 10 and 50^{0}C and was normally 20^{0}C. For a rise of 20^0 from room temperature of 27^{0}C, $\Lambda = 2 \times 10^{-3}$ sec^{-1}. Thus for exposures to pulses even as long as our maximum of 10 seconds, the heat losses may be neglected. Oscillographic traces of the calorimeter temperature showed the cooling curve slopes to be negligible, in agreement with this calculation. Broido and Willoughby further showed that for T small with respect to the exposure time, the temperature gradient across the thickness δ is small, and the measure of the rate of change of back surface temperature for a uniformly exposed receiver is a valid measure of the rate of change of the average temperature. For this receiver T is 0.0016 sec, while flux

measurements were made with exposure times from 0.030 to 10 sec. Thus $\Delta\theta/\Delta t$ can be measured at the back surface. $\Delta\theta/\Delta t$ was constant over the entire range of temperature rise and exposure time for each of the apertures, showing that heat conduction or convection from neighboring parts of the apparatus was negligible.

The received flux density in our case was not distributed uniformly over the receiver surface. This was because the flux density varied within the focal volume and, more importantly, the area receiving the flux which passed through the aperture was in general smaller than the total surface area of the receiver. Thus it was necessary to show that the temperature measured by the thermocouple at the edge of the calorimeter, θ_E, was to good approximation the average temperature θ_{AV}. This can be tested by considering the problem of a disk of diameter R_1 and thickness δ, heated over a circular area of radius $R_2 < R_1$.

The flow of heat in such a circular disk is represented by the following differential equation where it is assumed that the disk is sufficiently thin that only a radial flow exists:

$$\theta_t = \frac{a\, I_{R_2}}{\rho\, c\, \delta}\, H(R_2-r)\, H(\tau-t) + \kappa\left[\theta_{rr} + \frac{1}{r}\,\theta_r\right] \qquad (4)$$

with $\theta = 0$ at $t = 0$

$\theta_r = 0$ at $r = 0,\ R_1$,

and $$H(x) = \begin{cases} 1 & x > 0 \\ 0 & x < 0 \end{cases}$$

Here t and r are time and radial independent variables and the subscripts t and r indicate partial derivatives. τ is exposure time

and I_{R_2} is the flux density at the calorimeter over the circle of radius R_2. Equation (4) is solved by reducing it to two partial differential equations:

$$\theta_t = \kappa\left(\theta_{rr} + \frac{1}{r}\,\theta_r\right) \qquad \text{for} \quad R_2 < r \leq R_1 \tag{5}$$

with $\theta = 0 \quad \text{at} \quad t = 0$

$\theta_r = 0 \quad \text{at} \quad r = R_1$

and

$$\theta_t = \frac{a\, I_{R_2}}{\rho\, c\, \delta}\, H(\tau - t) + \kappa\left(\theta_{rr} + \frac{1}{r}\,\theta_r\right) \qquad \text{for} \quad 0 \leq r < R_2 \tag{6}$$

with $\theta = 0 \quad \text{at} \quad t = 0$

$\theta_r = 0 \quad \text{at} \quad r = 0$.

On taking the Laplace transform

$$\bar{\theta}(s,\, r) = \int_0^\infty e^{-st}\, \theta(t,\, r)\, dt \tag{7}$$

of Equations (5) and (6) along with their boundary conditions, one obtains the following ordinary differential equations in the variable r :

$$s\bar{\theta} = \kappa\left(\bar{\theta}_{rr} + \frac{1}{r}\,\bar{\theta}_r\right), \qquad R_2 < r \leq R_1 \tag{8}$$

with $\bar{\theta}_r = 0 \quad \text{at} \quad r = R_1$,

and

$$s\bar{\theta} = \frac{a\, I_{R_2}}{\rho\, c\, \delta}\,\frac{(1 - e^{-s\tau})}{s} + \kappa\left(\bar{\theta}_{rr} + \frac{1}{r}\,\bar{\theta}_r\right), \qquad 0 \leq r < R_2 \tag{9}$$

with $\bar{\theta}_r = 0 \quad \text{at} \quad r = 0$.

Define $q^2 = \frac{s}{\kappa}$ and $\alpha = \frac{a\, I_{R_2}}{\kappa\, \rho\, c\, \delta}\,\frac{1 - e^{-s\tau}}{s}$. Then the solutions[4] of Equations (8) and (9) are

$$\bar{\theta} = C_1 \left[I_0(qr) + \frac{I_1(qR_1)}{K_1(qR_1)} K_0(qr) \right] , \quad R_2 < r \leq R_1 \qquad (10)$$

$$\bar{\theta} = \frac{\alpha}{q^2} + C_2 I_0(qr) , \quad 0 \leq r < R_2 \qquad (11)$$

where C_1 and C_2 are arbitrary constants and I_n and K_n are the solutions of the modified Bessel equation. The constants, C_1 and C_2, are determined by applying the further conditions that $\bar{\theta}$, $\bar{\theta}_r$ in (10) and (11) must agree identically at $r = R_2$. Equations (10) and (11) become

$$\bar{\theta} = \frac{\alpha R_2}{q} \frac{I_1(q R_2)}{I_1(q R_1)} \left[I_0(qr) K_1(q R_1) + I_1(q R_1) K_0(qr) \right]$$
$$R_2 < r \leq R_1 \qquad (12)$$

and

$$\bar{\theta} = \frac{\alpha}{q^2} + \frac{\alpha R_2}{q} \frac{I_0(qr)}{I_1(qR_1)} \left[I_1(q R_2) K_1(q R_1) - I_1(q R_1) K_1(q R_2) \right]$$
$$0 \leq r < R_2 . \qquad (13)$$

Set $r = R_1$ in Equation (12) and $r = 0$ in Equation (13). Then

$$\bar{\theta} = \frac{\alpha}{q^2} \frac{R_2}{R_1} \frac{I_1(q R_2)}{I_1(q R_1)} \quad \text{at the edge} \qquad (12a)$$

and

$$\bar{\theta} = \frac{\alpha}{q^2} + \frac{\alpha R_2}{q} \left[I_1(q R_2) \frac{K_1(q R_1)}{I_1(q R_1)} - K_1(q R_2) \right] \quad \text{at the center.} \qquad (13a)$$

Laplace inversion[5] of Equations (12a) and (13a) gives integrals which may be evaluated using Cauchy's theorem of residues.[6] Let $R = R_2/R_1$. Define

$$\varphi(t, R_1) = \frac{a I_{R_2}}{\rho c \delta} \left[R^2 \frac{(R_2^2 - R_1^2)}{8\kappa} + R^2 t - 2 R \Sigma_E \right] \qquad (14)$$

and

$$\varphi(t, 0) = \frac{a I_{R_2}}{\rho c \delta} \left[- \frac{R_2^2}{2\kappa} \ln R + R^2 \frac{(R_2^2 - R_1^2)}{8\kappa} + R^2 t - 2R\Sigma_C \right] \qquad (15)$$

where

$$\Sigma_E(t) = \sum_{i=1}^{\infty} \frac{e^{-\kappa\alpha_i^2 t}}{\kappa\alpha_i^2} \frac{J_1(\alpha_i R_2)}{\alpha_i R_1 J_0(\alpha_i R_1)}$$

and

$$\Sigma_C(t) = \Sigma_E(t) + \sum_{i=1}^{\infty} \left\{ \frac{e^{-\kappa\alpha_i^2 t}}{\kappa\alpha_i^2} \frac{J_1(\alpha_i R_2)}{J_0(\alpha_i R_1)} \cdot \alpha_i R_1 \sum_{r=0}^{\infty} \frac{(-1)^r \left|\frac{\alpha_i R_1}{2}\right|^{2r}}{r!\,(r+1)!} \left[\sum_{m=1}^{r+1} \frac{1}{m} + \sum_{m=1}^{r} \frac{1}{m} \right] \right\},$$

and J_0, J_1 are the ordinary Bessel functions. The α_i are the non-negative solutions of $J_1(\alpha R_1) = 0$. Then

$$\theta(t, R_1) = \varphi(t, R_1) - H(t-\tau)\,\varphi(t-\tau, R_1) \qquad (16)$$

$$\theta(t, 0) = \varphi(t, 0) - H(t-\tau)\,\varphi(t-\tau, 0)\,. \qquad (17)$$

Assume $t - \tau < 0$. Then Equations (16) and (17) become

$$\theta(t, R_1) = \varphi(t, R_1) = \theta_E \quad \text{at the edge} \qquad (16a)$$

$$\theta(t, 0) = \varphi(t, 0) \quad \text{at the center}\,. \qquad (17a)$$

At time t, the average temperature of the disk is given by

$$\theta_{AV}(t) = \frac{a I_{R_2} R^2 t}{\rho c \delta}\,. \qquad (18)$$

The ratio of the temperature at the edge of the disk to the average temperature at any time, t, is found by combining Equations (14), (16a), and (18) to give

$$\theta_R = \frac{\theta_E}{\theta_{AV}} = 1 - \frac{R_1^2 - R_2^2}{8\kappa t} - \frac{2\Sigma_E(t)}{Rt}\,. \qquad (19)$$

Note that $\lim_{t\to\infty} \Sigma_E(t) = 0$. It is therefore possible to find a t_0 such that $\theta_R \cong \bar{\theta}_R$ as closely as desired for all $t \geq t_0$ where

$$\bar{\theta}_R = 1 - \frac{R_1^2 - R_2^2}{8 \kappa t} . \qquad (20)$$

The arc length along a geodesic line across the calorimeter surface is 0.828 cm. For an aperture diameter of 0.25 cm the arc length subtended by the beam is 0.604 cm. In approximation take $R_1 = 0.414$ cm and $R_2 = 0.302$ cm. For a typical case with this aperture $I_a = 20$ cal/cm^2-sec, and $\Delta t = 1.17$ seconds for $\Delta\theta = 20^0$C. From Equation (20) $\bar{\theta}_R = 0.992$ for $\kappa = 1.095$ cm^2/sec. Considerations of the asymptotic forms for the Bessel functions and inspection of the leading terms allow one to bound the series $\Sigma_E(t)$ so that

$$\theta_R - \bar{\theta}_R = - \frac{2\Sigma_E(t)}{t R} < e^{-100} \qquad \text{at} \quad t = 1.17 \text{ sec.}$$

Thus the error in approximating θ_R by $\bar{\theta}_R$ in this case is negligible and the measurement of temperature at the edge of the calorimeter gives a good approximation to the average temperature.

In summary the analysis shows that the average flux density at the plane of the aperture and over the aperture area may be calculated from Equation (1), where $\Delta\theta_{AV}/\Delta t$ is to good approximation the rate of temperature rise at the thermocouple.

3. Flux Density Distribution in the Focal Volume

Flux density in the focal volume was mapped by traversing along axial, horizontal, and vertical axes with constant apertures in the range 0.025 to 0.508 cm in diameter. In further experiments the calorimeter was centered at a selected point, and the flux density was measured for different apertures over the same range. Figure 3 shows flux density

normalized by maximum flux density, as a function of vertical, horizontal, and axial distance from the point of maximum flux. The aperture was 0.127 cm. For the horizontal traverse, points for an aperture of 0.064 cm are also shown; the shape of the surfaces of constant flux density was the same for each aperture. The dispersion is believed due chiefly to wandering of the arc and hence of the image over the aperture.

A typical curve of measured flux density versus aperture diameter, with the calorimeter in this case centered at the point of maximum flux density, is given in Fig. 4. For aperture diameters smaller than 0.250 cm the apparent flux density rises sharply. Since for all apertures the flux density drops off as one moves away from the maximum at the focal volume center, the increase in apparent flux density with decrease in aperture at given calorimeter position must be related to aperture thickness. At an aperture of 0.250 cm the aperture thickness begins to be a significant fraction of the radius, the ratio being 0.1. A thickness-related increase in apparent flux density can arise from reflections from the walls of an aperture placed in a focal volume. From geometric optics it is clear that proper placing of a thick aperture within the focal volume can substantially increase the flux passing through the aperture above the amount which would pass if the shield were infinitely thin. Auxiliary experiments confirmed that apparent flux density was dependent on foil thickness at small apertures.

The data, which include Figs. 3 and 4 as well as traverses with larger apertures, are consistent under the assumption that effects due to reflection from the wall of the aperture are negligible at apertures of 0.25 cm

normalized by maximum flux density, as a function of vertical, horizontal, and axial distance from the point of maximum flux. The aperture was 0.127 cm. For the horizontal traverse, points for an aperture of 0.064 cm are also shown; the shape of the surfaces of constant flux density was the same for each aperture. The dispersion is believed due chiefly to wandering of the arc and hence of the image over the aperture.

A typical curve of measured flux density versus aperture diameter, with the calorimeter in this case centered at the point of maximum flux density, is given in Fig. 4. For aperture diameters smaller than 0.250 cm the apparent flux density rises sharply. Since for all apertures the flux density drops off as one moves away from the maximum at the focal volume center, the increase in apparent flux density with decrease in aperture at given calorimeter position must be related to aperture thickness. At an aperture of 0.250 cm the aperture thickness begins to be a significant fraction of the radius, the ratio being 0.1. A thickness-related increase in apparent flux density can arise from reflections from the walls of an aperture placed in a focal volume. From geometric optics it is clear that proper placing of a thick aperture within the focal volume can substantially increase the flux passing through the aperture above the amount which would pass if the shield were infinitely thin. Auxiliary experiments confirmed that apparent flux density was dependent on foil thickness at small apertures.

The data, which include Figs. 3 and 4 as well as traverses with larger apertures, are consistent under the assumption that effects due to reflection from the wall of the aperture are negligible at apertures of 0.25 cm

and greater. They depict an image with roughly ellipsoidal surfaces of constant flux, the maximum flux density being at the center. The flux density falls off to 97-99% of maximum at 0.05 cm from the center, and to 88-95% of maximum at 0.125 cm from center. The maximum value is 5% higher than that measured by the 0.250-cm aperture centered at the focal center.

Acknowledgments: Mr. I. A. Illing performed the experimental measurements. Thanks are due to numerous others for suggestions and cooperation. Among these are Dr. C. P. Butler of the U. S. Naval Radiological Defense Laboratory in San Francisco; Dr. John H. Hett of Hett Associates, Inc., Cresskill, N. J.; and Dr. C. M. Ablow, Mr. Norman Fishman and Dr. Henry Wise of Stanford Research Institute.

REFERENCES

1. M. R. Null and W. W. Lozier, Rev. Sci. Instr. 29, 163 (1958)
2. N. K. Hiester and R. E. De La Rue, ARS Journ. 30, 928 (1960)
3. A. Broido and A. B. Willoughby, J. Opt. Soc. Am. 48, 344 (1958)
4. H. S. Carslaw and J. C. Jaeger, Conduction of Heat in Solids, Oxford University Press, 2nd Edition, 1959, Appendix III.
5. Reference 4, Appendix I
6. See for instance E. T. Copson, An Introduction to the Theory of Functions of a Complex Variable, Oxford at the Clarendon Press, 1st Edition, 1935, p. 117

FIGURE TITLES

1. Sketch of double ellipsoidal arc image furnace system.
2. Calorimeter for calibrating radiant flux density.
3. Flux density divided by maximum flux density versus distance from center of focal volume.
4. Apparent flux density at center of focal volume versus aperture diameter.

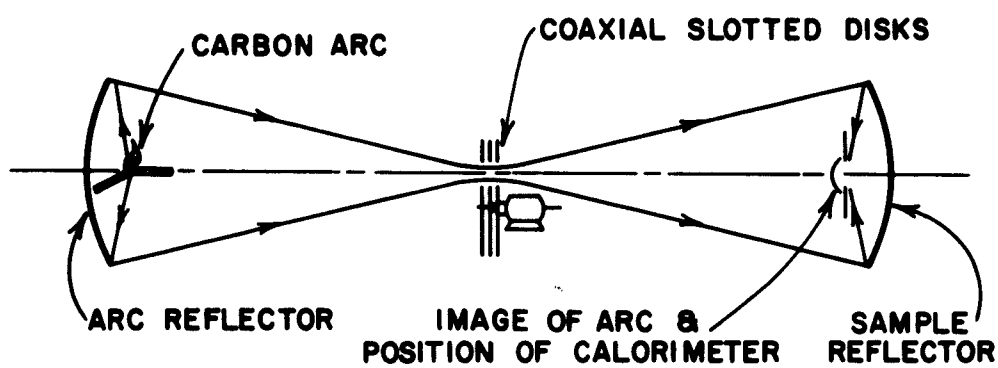

FIG. 1 SKETCH OF DOUBLE ELLIPSOIDAL ARC IMAGE FURNACE SYSTEM

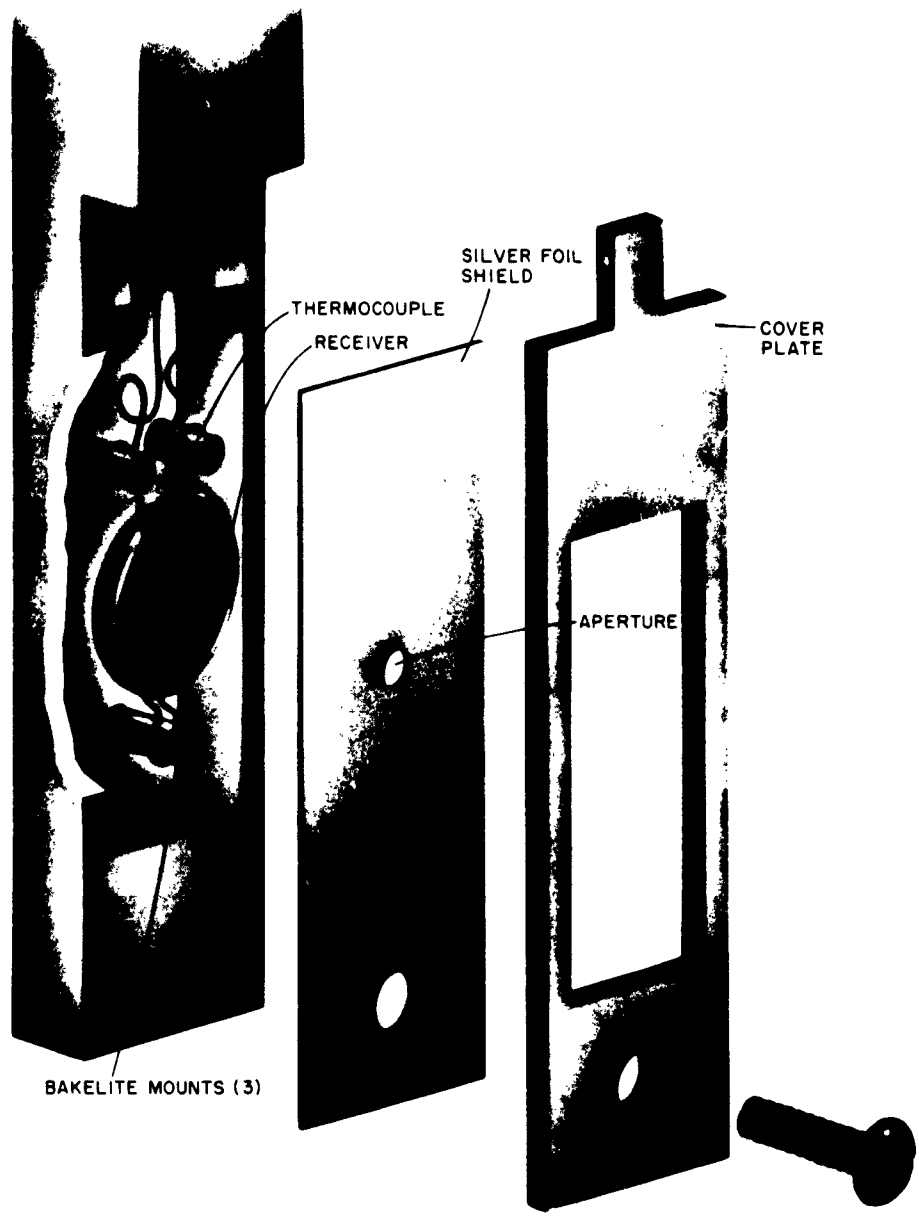

FIG. 2 CALORIMETER FOR CALIBRATING RADIANT FLUX DENSITY

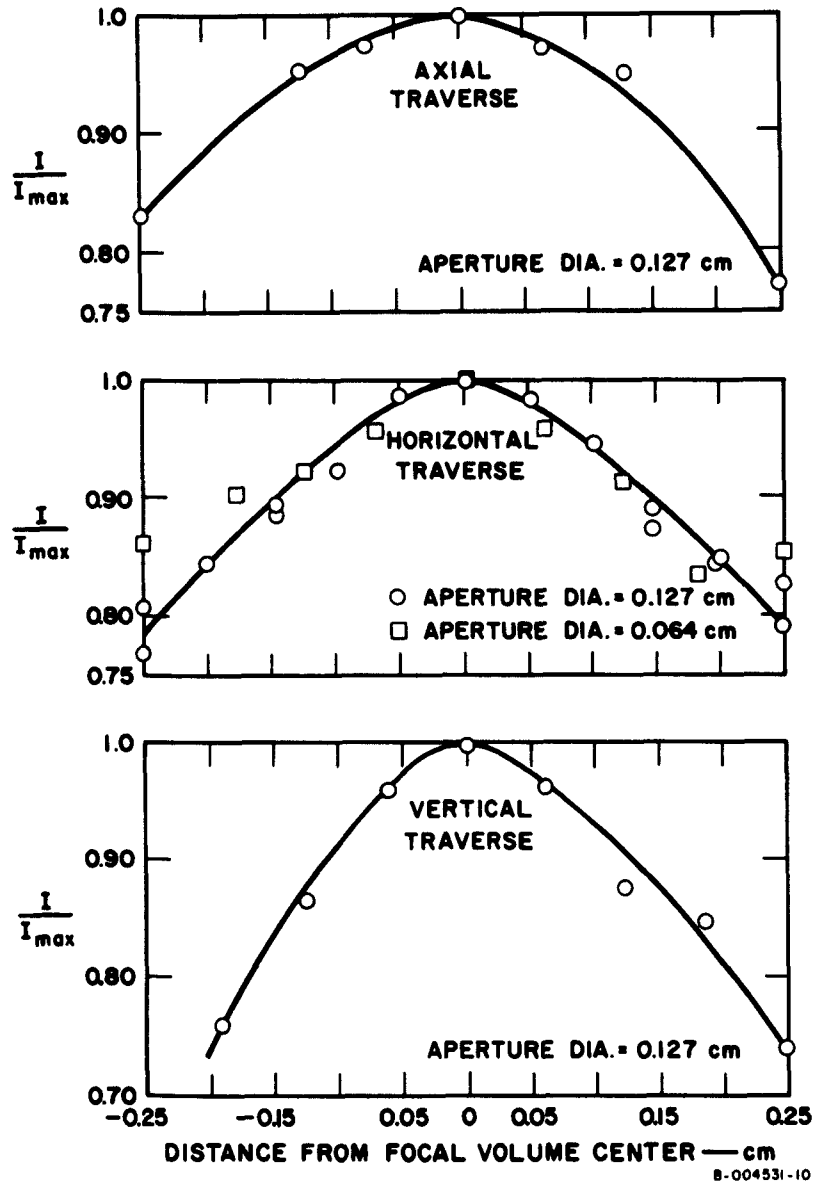

FIG. 3 FLUX DENSITY DIVIDED BY MAXIMUM FLUX DENSITY VERSUS DISTANCE FROM CENTER OF FOCAL VOLUME

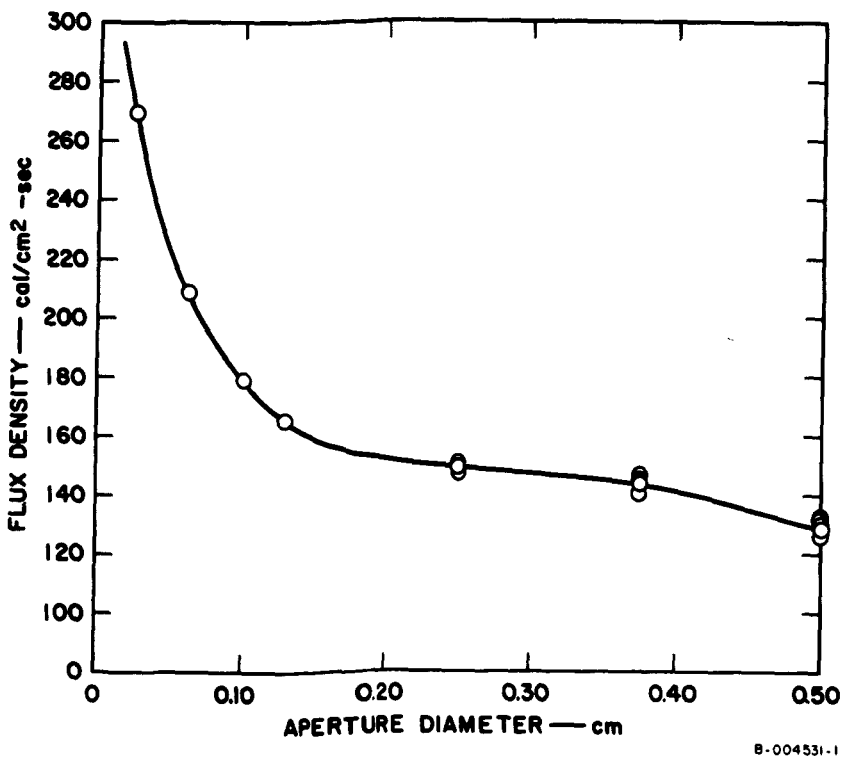

FIG. 4 APPARENT FLUX DENSITY AT CENTER OF FOCAL VOLUME VERSUS APERTURE DIAMETER